Mass spectrometry and theoretical investigation of di-alkylphosphoric acid–lanthanide complexes

E. Leclerc, D. Guillaumont, Philippe Guilbaud, L. Berthon

Radiochim. Acta **96**, 85–92 (2008) / **DOI** 10.1524/ract.2008.1466

Mass spectrometry and theoretical investigation of di-alkylphosphoric acid–lanthanide complexes

By E. Leclerc, D. Guillaumont, P. Guilbaud and L. Berthon*

CEA Valrhô, DEN/DRCP/SCPS, B.P. 17171, 30207 Bagnols-sur-cèze Cedex, France

(Received May 16, 2007; accepted in revised form August 10, 2007)

Electrospray ionization / Mass spectrometry / Dialkylphosphoric acid / Lanthanide / Quantum chemistry / Molecular dynamics

Summary. In the framework of nuclear waste reprocessing, separation processes of minor actinides from fission products are developed using liquid–liquid extraction. In order to understand the mechanism involved in the extraction process, complexes with lanthanide cations and di-(2-ethylhexyl) phosphoric and di-*n*-hexyl phosphoric acids have been characterized using a combination of mass spectrometric methods, molecular dynamic simulations and quantum chemistry calculations.

Introduction

The minor actinides An(III) are responsible for the majority of the long lasting radiotoxicity in waste from the PUREX reprocessing of used nuclear fuel [1]. To improve the management of radioactive wastes, CEA (Commissariat à l'Energie Atomique) has undertaken the development of a liquid–liquid extraction process which has the objective, in particular, to separate the minor actinides An(III) from the high-level liquid waste. After their removal, the An(III) can be transmuted by neutron bombardment to short lived radionuclides [2]. The separation of An(III) (americium and curium) from the lanthanides(III) is an essential step prior to the transmutation of the actinides because lanthanide absorb neutrons very effectively. In this frame, the CEA developed the DIAMEX (Diamide Extraction) – SANEX (Selective Actinide Extraction) process [3, 4]. In this process, the raffinate from the PUREX process is contacted with a mixture of a malonamide and a di-alkylphosphoric acid diluted in an appropriate aliphatic diluent. Under highly acidic conditions (~ 3 M HNO_3) of the aqueous phase, both An(III) and Ln(III) are co-extracted by the malonamide [5, 6]. The separation/recovery of An(III) is then accomplished by contacting the loaded organic phase with an aqueous phase containing a complexing agent of actinides(III) in a low acidity aqueous phase [7]. Under these conditions the diamide is completely ineffective as an extractant for metal cations, while the organophosphoric acid exhibits efficient extraction and significant selectivity for Ln(III) over An(III) [8]. Several di-alkylphosphoric acids such as di-2-ethylhexylphosphoric acid (HDEHP) and di-*n*-hexylphosphoric acid (HDHP) (Fig. 1) have been proposed for this process [7, 9].

The present work deals with the extraction of trivalent lanthanides in low acidity aqueous phase by di-2-ethylhexylphosphoric acid (HDEHP) and di-*n*-hexylphosphoric acid (HDHP) diluted in dodecane. Many fundamental studies on the extraction of actinides and lanthanides by di-alkylphosphoric acid have been published [10–14], reporting values for the acid dissociation, distribution and dimerization constants of di-alkylphosphoric acids in various diluents. The main features of metal solvent extraction by dialkylphosphoric acids are the formation of highly stable hydrogen-bonded dimers in alkane diluents [12–18], and the extraction of metal ions (M^{x+}) by the dimerized extractant according to the general cation-exchange stoichiometry:

$$M^{x+} + x\overline{(LH)_2} \leftrightarrow \overline{M(LH\,L)_x} + xH^+ ,$$

where the bar denotes organic phase species, HL and L are the dialkylphosphoric acid and the deprotonated acid, respectively, and x represents the cation charge.

Complexes formed in organic phase after extraction of lanthanides or actinides by HDEHP or HDHP have been investigated through various experimental approaches such as IR [7, 19], VPO [7], SANS [7, 19] and absorption spectroscopy [19, 20] (UV-visible, EXAFS ...). However, no studies have been reported so far using electrospray ion-

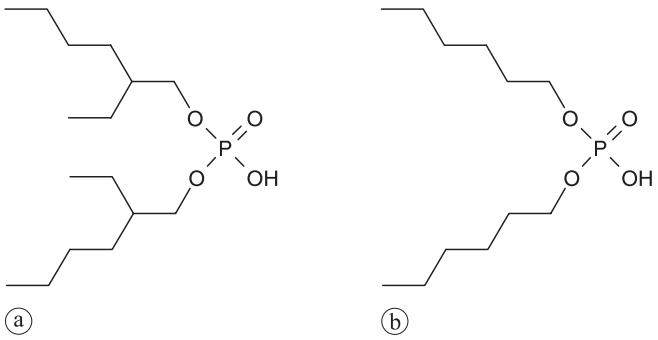

Fig. 1. Schematic representation of HDEHP (**a**) and HDHP (**b**) chemical structures.

*Author for correspondence (E-mail: laurence.berthon@cea.fr).

isation mass spectrometry (ESI-MS) to characterize these complexes. Electrospray ionisation mass spectrometry is a relatively recent tool for studying metal–ligand interactions [21–24], it has been shown to be an appropriate technique to characterize ions in solution and has been used to identify the coordination sphere of complexes. An advantage of this technique is its ability to determine the stoichiometry of the complexes in solution and to investigate their stability in the gas phase [23, 25–29]. However, the use of ESI-MS has been mostly restricted to ion complexation studies and despite its advantages, the use of this approach for solvent extraction studies remain rare [30, 31].

We report here the characterisation of lanthanides–dialkylphosphoric acid complexes in the gas phase using a combination of mass spectrometric methods and theoretical chemistry calculations (molecular dynamics simulations and quantum chemistry). The influence of the structure of the extractant on the stability of the complexes is discussed.

Experimental and theoretical methods

Reagents

HDEHP was provided by the BDH Chemical Company and had > 98% purity. HDHP was synthesized in our laboratories with purity higher than of 99% [32]. The diluent *n*-dodecane was a Sigma-Aldrich (Lyon, France) with a purity of 99%.

HDEHP and HDHP were diluted in dodecane to the appropriate concentration. Stocks solutions (5×10^{-2} mol L^{-1}) of lanthanide(III) were prepared by dissolving crystals of $Ln(NO_3)_3 \cdot nH_2O$ ($n = 5$ or 6) (Sigma-Aldrich) in glycolic acid aqueous phase at pH 3. All chemicals were of reagent grade and Millipore water was used throughout the procedure.

Extraction

The HDEHP and HDHP mass spectra were realized using a 0.15 mol L^{-1} solution diluted in dodecane. Extraction experiments with lanthanide were realized with the following conditions. 1 mL of di-alkylphosphoric acid diluted in dodecane is contacted with 4 mL of glycolic acid aqueous phase at pH 3 containing 0.01 mol/L of lanthanide.

Electrospray ionization – mass spectrometry

The mass spectrometric measurements were recorded in positive ionization mode using a Bruker Esquire-LC quadrupole ion trap equipped with an electrospray interface. The capillary voltage was set to 4 kV in positive ionization mode. Nitrogen operating at 5 L min^{-1} was employed as drying gas and at 5 psi for nebulizing gas. Samples were diluted in ethanol to 1/10 and then in CH_3CN/H_2O (1 : 1 v/v) to 1/100. A syringe infusion pump (Cole Parmer) delivered the sample at 60 μL h^{-1} to the electrospray source. The source temperature was set to 250 °C. The sample cone voltage was optimized at 30 V. Spectra were acquired over a mass range of m/z 45–2200. The energy resolved mass spectrometry experiments were performed by cone voltage (skimmer 1) variation between 20 to 100 V, the skimmer 2 voltage is kept constant at 10 V.

Quantum chemistry calculations

The fragmentation mechanism was investigated through quantum chemistry calculations for the free ligands and for the complex of europium with four ligands ($[Eu(LH)_2(L)_2]^+$) by determining the structures and energy of the reactants, products and transition states. In the calculations on $[Eu(LH)_2L_2]^+$, three of the four ligands have been modeled by di-methylphosporic acid. In the calculations on the free ligands, one of the two alkyl chains was modeled by a methyl group.

Geometry optimizations of all intermediate complexes and transition states were carried out using the B3LYP functional with the Gaussian98 package [33], relativistic effects were considered through the use of relativistic effective core potentials (RECP) developed in the Stuttgart and Dresden groups [34]. Large-core RECP was used with the accompanying basis set to describe the valence electron density, $7s6p5d$ contracted to $5s4p3d$. On other atoms a 6–31 G* basis was employed for geometry optimization and frequency calculations. Additional single point energy calculations were performed on the optimized geometry using a larger $6-311+G(d, p)$ basis set.

The geometries of all the complexes were fully optimized without any symmetry constraint and vibrational frequencies were calculated analytically.

Molecular dynamics calculations

Molecular Dynamics (MD) simulations were performed using the AMBER6 software [35], using the following representation of the potential energy :

$$E = \sum_{\text{bonds}} K_r (r - r_{\text{eq}})^2 + \sum_{\text{angles}} K_\theta (\theta - \theta_{\text{eq}})^2 + \sum_{\text{dihedrals}} V_n [1 + \cos(n\phi - \phi_0)] + \sum_{i=1}^{N-1} \sum_{j>i}^{N} \left[\frac{A_{ij}}{R_{ij}^{12}} - \frac{B_{ij}}{R_{ij}^{6}} + \frac{q_i q_j}{R_{ij}} \right].$$

Lennard–Jones parameters for Eu^{3+} were adjusted upon both hydration geometries and $\Delta\Delta G$s of La^{3+}, Eu^{3+} and Lu^{3+} cations [36]. Charges on organic ligands have been adjusted using RESP [37] to represent the electrostatic potentials obtained from HF/6–31 G* calculations with Gaussian98.

All studied systems were equilibrated for at least 100 ps by raising temperature from 100 to 300 K. MD simulations were then carried out for 500 ps in order to obtain Potential of Mean Force (PMF) starting points. PMF calculations have been performed using the Free Energy Perturbation (FEP) Window Growth included in GIBBS (AMBER) module. The free energy is calculated at discrete and uniformly spaced intervals of λ using these formulae:

$$G_{\lambda(i+1)} - G_{\lambda(i)} = -RT \ln\langle \exp -[(V_{\lambda(i+1)} - V_{\lambda(i)})/RT] \rangle_{\lambda(i)}$$

and

$$\Delta G = G_1 - G_0 = \Sigma (G_{\lambda(i+1)} - G_{\lambda(i)}) ,$$

where G_0 and G_1 are the free energies of states 0 and 1, respectively, $V_{\lambda(i)}$ is the potential energy function representative of state $\lambda(i)$, and $\langle\rangle_{\lambda(i)}$ the ensemble average of the

Table 1. m/z ratio and assignment of Ln–dialkyl phosphoric acid species detected in ESI-MS. Ln represents the lanthanide cation and LH the dialkyl phosphoric acid.

	Based peak m/z (width of pattern)			
	HDEHP-Nd	HDEHP-Eu	HDHP-Nd	HDHP-Eu
$Ln(LH)_2L_2^+$	1431.2 (1428.8–1437.3)	1440.1 (1438.1–1442.2)	1206.8 (1204.7–1214.0)	1215.6 (1213.6–1217.6)
$Ln(LH)_3L_2^+$	1753.3 (1751.0–1759.3)	1762.2 (1760.2–1764.2)	1472.9 (1470.8–1214.0)	1480.1 (1479.3–1483.7)
$Ln(L-H)_2L_4^+$	2075.1 (2073.3–2081.9)	2084.1[a] (2082.3–2086.2)	1738.4 (1736.6–1746.4)	1746.2[a] (1743.2–1750.0)

[a] the intensity of these peaks are very low.

enclosed quantity, representative of state $\lambda(i)$. The ensemble is evaluated from an MD trajectory run with $V = V_{\lambda(i)}$.

Results and discussion

Electrospray mass spectrometry

Europium and neodymium extraction have been investigated for both HDEHP and HDHP in dodecane. The positive ionization mode mass spectra of the organic phase were carried out. The assignment of the lanthanides complexes are reported in Table 1. The mass spectrum of the organic phase of neodymium with HDEHP is presented on Fig. 2 and is very similar to the mass spectrum obtained with HDHP.

The presence of di-alkylphosphoric acid–lanthanide complexes and 'free' dialkylphosphoric acid (monomer and multimers protonated or associated with Na^+ or K^+ ions present in solution) are observed. For both extractants, three complexes have been identified as $[Ln(LH)_2L_2]^+$, $[Ln(LH)_3L_2]^+$ and $[Ln(LH)_4L_2]^+$. In the case of the europium extraction, the last complex corresponding to $[Eu(LH)_4L_2]^+$ has a lower intensity (0.5%).

In order to understand the structure of the complex and the fragmentation mechanism, the fragmentation spectra were recorded for $[Nd(LH)_2L_2]^+$, $[Nd(LH)_3L_2]^+$ and $[Nd(LH)_4L_2]^+$.

With HDEHP, the fragmentation spectrum of $[Nd(LH)_4L_2]^+$ leads to two ions which are assigned to $[Nd(LH)_3L_2]^+$ and $[Nd(LH)_2L_2]^+$ (Fig. 3). For $[Nd(LH)_3L_2]^+$, an ion is observed and assigned to $[Nd(LH)_2L_2]^+$. In contrast, with $[Nd(LH)_2L_2]^+$, two major fragmentation pathways are observed. The first path leads to an ion at 1108.7 and corresponds to the loss of one ligand (−322), as observed with $[Nd(LH)_3L_2]^+$ and $[Nd(LH)_4L_2]^+$. The second path leads to an ion with a mass signal of smaller intensity and corresponds to the loss of one alkyl chain (−112). Other fragmentations are observed and correspond to the consecutive loss of the alkyl chain (Fig. 4). With europium, the same fragmentations are observed but on the collision spectra of the complex with four ligands

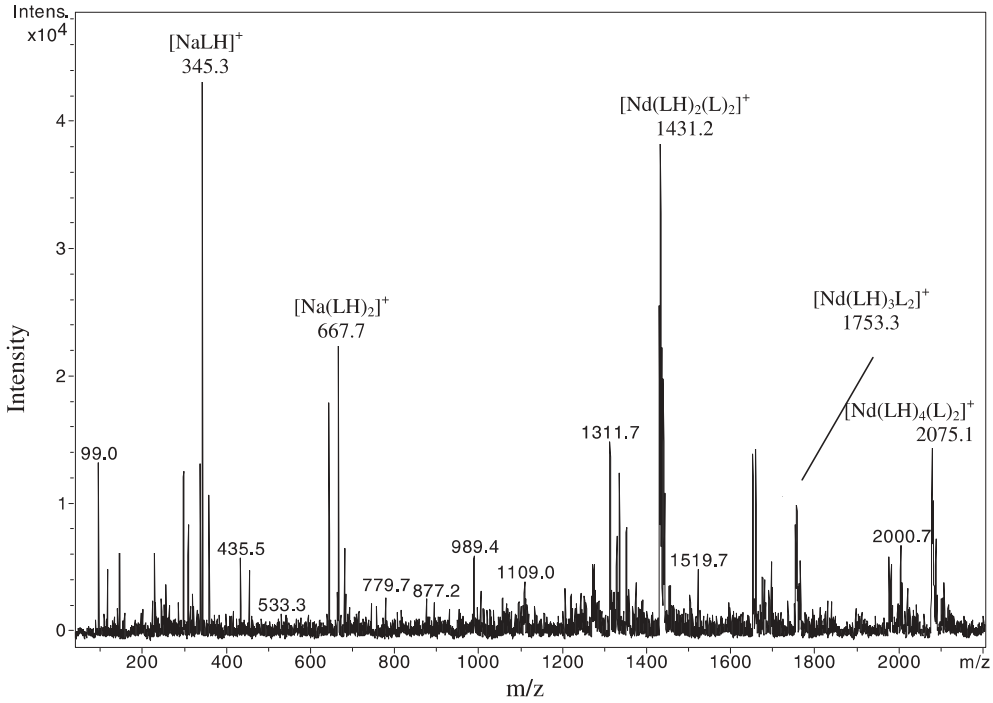

Fig. 2. Positive ESI mass spectrum of organic phase of HDEHP in *n*-dodecane after extraction of Nd. LH corresponds to HDEHP. The peak at m/z = 99.0 are assigned to H_3PO_4 protonated arising by fragmentation of HDEHP during the ionization process; the peak at m/z = 345.3; 645,6; 667,7; 1311,7; 1333.8; 1650.4 are assigned to $[Na(LH)]^+$, $[H(LH)_2]^+$, $[Na(LH)_2]^+$, $[Na(LH)_4]^+$, $[Na(LH)_3(LNa)]^+$, $[K(LH)_5]^+$.

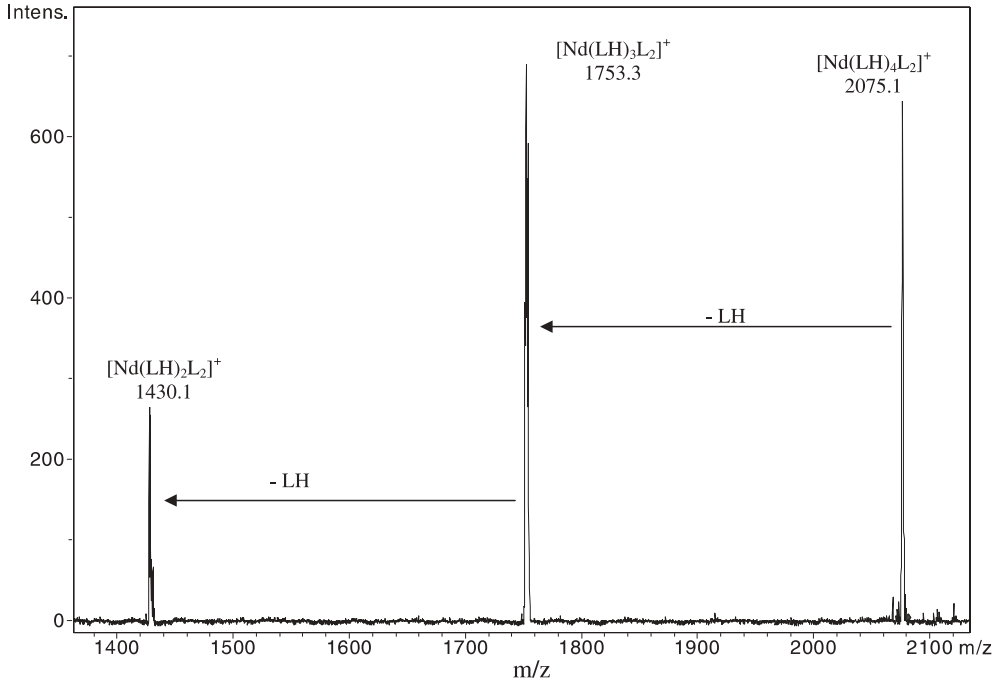

Fig. 3. MS^2 spectrum of $[Nd(LH)_4L_2]^+$ complex observed in organic phase of HDEHP in *n*-dodecane after extraction of Nd. Fragmentation amplitude: 0.80 V. LH corresponds to HDEHP.

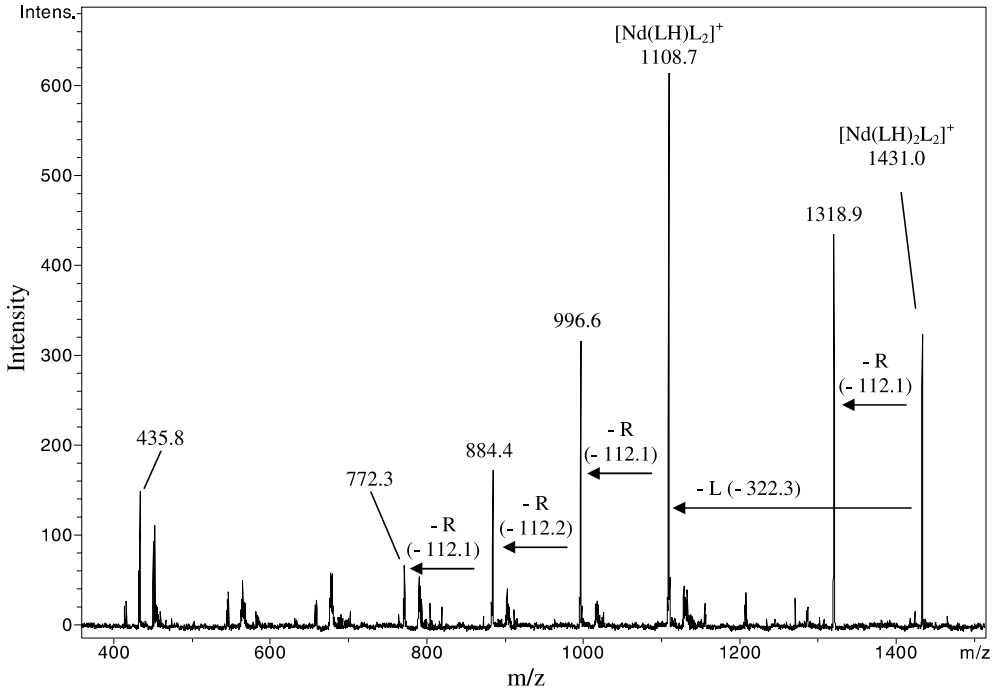

Fig. 4. MS^2 spectrum of $[Nd(LH)_2L_2]^+$ complex observed in organic phase of HDEHP in *n*-dodecane after extraction of Nd. Fragmentation amplitude: 1.25 V. LH corresponds to HDEHP. The peak at $m/z = 345.3$ correspond to a complex which has lost all alkyl chain.

$[Eu(LH)_2L_2]^+$, the intensity of the two major ions is inverted (loss of one ligand and one alkyl chain).

With HDHP, for the complex with six ligands $[Nd(LH)_4L_2]^+$, three ions are observed which are assigned to $[Nd(LH)_3L_2]^+$, $[Nd(LH)_2L_2]^+$ and $[Nd(LH)L_2]^+$. These ions correspond to the consecutive loss of a ligand. As observed with HDEHP, no alkyl chain loss was detected. $[Nd(LH)_3L_2]^+$ leads also to the loss of a ligand. For the last complex $[Nd(LH)_2L_2]^+$, the ligand elimination is the major pathway. Contrary to HDEHP, the alkyl chain loss is not observed. But as obtained with HDEHP, $[Nd(LH)L_2]^+$ leads to consecutive eliminations of alkyl chain. The same results were obtained for the europium complexes.

These results show that the metal is surrounded by 6 ligands, which agrees with the previous studies carried out by liquid–liquid extraction and EXAFS [7, 14, 19, 20]. In addition, the spectra show that the most stable complex in the gas phase has four ligands strongly bonded to the lanthanide cation. Energy resolved mass spectrometry experiments by cone voltage variation were performed with Eu-HDHP system and had also shown that the most stable complex is $[Eu(LH)_2L_2]^+$. Indeed, the intensity of the parent ion de-

creases at higher cone voltage: the maximum of intensity of $[Ln(LH)_4L_2]^+$, $[Ln(LH)_3L_2]^+$, $[Ln(LH)_3L_2]^+$ are observed at 30 V, 50 V and 70 V respectively.

In solution, the complex is probably $Ln(LH)_3L_3$ which is globally neutral. During the ionization process and the transfer in the gas phase, this species is modified and transformed into $[Ln(LH)_4L_2]^+$ by an addition of a proton to form a positive ion. The fragmentation of this ion shows that 2 ligands are less strongly bonded to the metal and the more stable species in the gas phase is $[Ln(LH)_2L_2]^+$. Two different fragmentation pathways of these last species are observed: loss of one ligand or fragmentation of an alkyl chain depending on the structure of the ligand.

Fragmentation mechanism

From the above results, we can conclude that two major different fragmentation paths may take place (Fig. 5):

– A first path (A) corresponds to the elimination of one ligand.

– A second path (B) corresponds to the loss of one alkyl chain. For this path, we propose a mechanism where the hydrogen atom bonded to the carbon atom in beta position from oxygen atom is attacked by the oxygen. This reaction leads to the formation of the corresponding alkene and to a new complex (III).

For complexes of higher stoichiometry, $[Ln(LH)_4L_2]^+$ and $[Ln(LH)_3L_2]^+$, only path A is observed for both ligands. Only the protonated ligand (HDEHP or HDHP) can be reasonably loss considering that the negatively charged deprotonated ligand ($DEHP^-$ or DHP^-) should be more tightly bound to the metal.

For $[Ln(LH)_2L_2]^+$ complexes, both path A and B are observed for HDEHP (Fig. 5) whereas only path A is observed for HDHP.

For $[Ln(LH)L_2]^+$ complexes path B becomes the major fragmentation path for both ligands.

Path A has been investigated using molecular dynamics PMF calculations for both (HDEHP and HDHP) ligands with $[Eu(LH)_nL_2]^+$ $(1 \leq n \leq 4)$ complexes. In all cases,

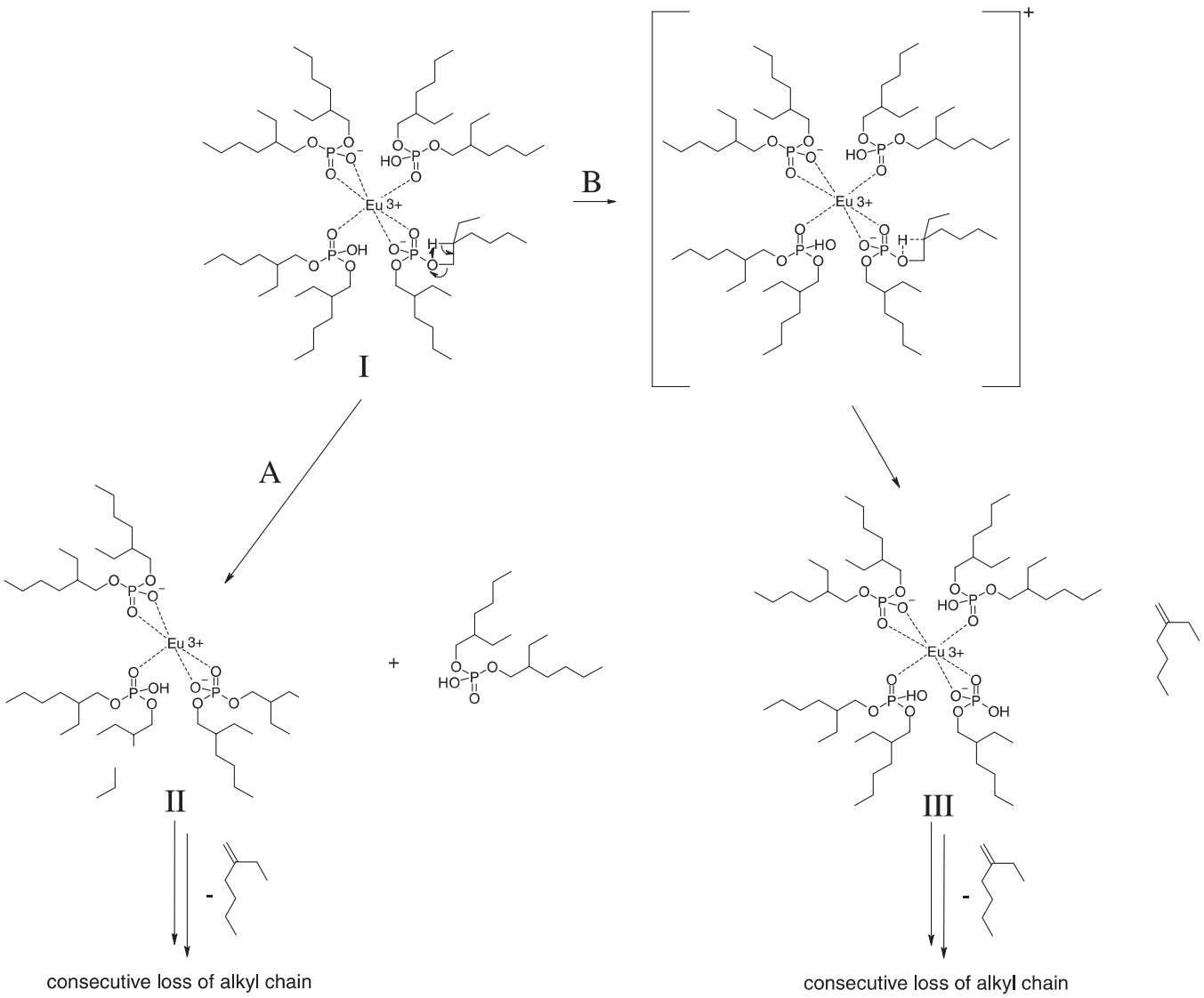

Fig. 5. Fragmentation pathways of $[Eu(LH)_2L_2]^+$ determined from mass spectrometry results. LH corresponds to HDEHP. Path A: elimination of one ligand leading to the complex II, Path B: loss of one alkyl chain leading to the formation of alkene and a complexe III.

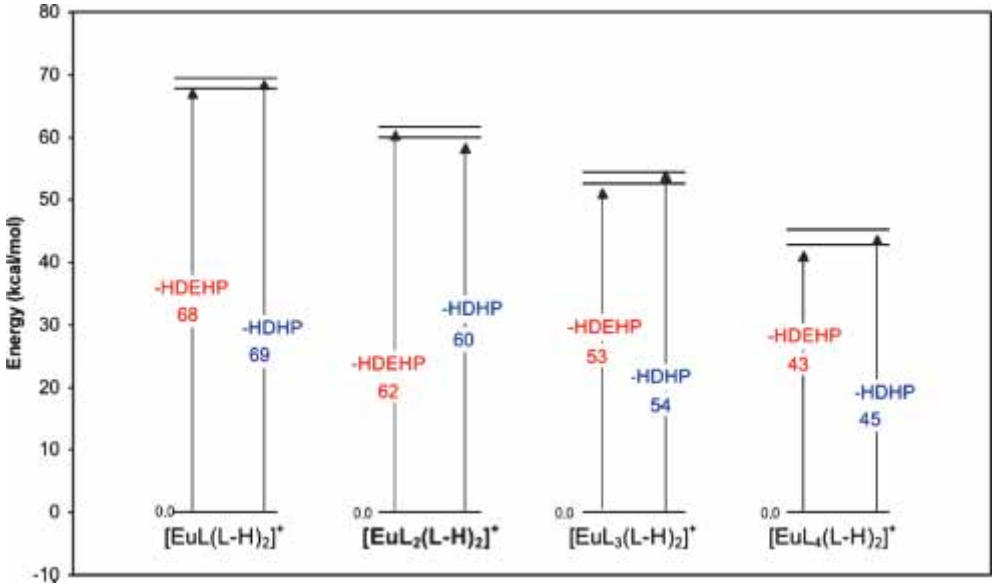

Fig. 6. Free energy perturbation $\Delta\Delta G$s, for $[EuL_n(L{-}H)_2]^+$ to $[EuL_{(n-1)}(L{-}H)_2]^+/L$ potential of mean force simulations (kcal/mol).

these calculations were performed for *forward* and *reverse* pathways, *i.e.* first starting with $[Eu(LH)_nL_2]^+$ and moving away one coordinated ligand LH at 20 Å from Eu^{3+} (leading to $[Eu(LH)_{(n-1)}L_2]^+/LH$), and then starting with this PMF calculation's last set, and bringing back the distant ligand in the cation first coordination sphere. $\Delta\Delta G$s given in Fig. 6 are averaged on these two calculations. Each of these sixteen Window Growth Free Energy Perturbation calculations lasted for between 2 and 3 simulated nanoseconds.

The elimination of one (protonated) ligand is calculated to be energetically equivalent for both HDEHP and HDHP at each $[Eu(LH)_nL_2]^+$ stoichiometry, in agreement with ESI-MS experiments. This removal is easier for bigger complexes, requiring about 10 kcal/mol less for each $[Eu(LH)_nL_2]^+$ complex compared to the following $[Eu(LH)_{(n-1)}L_2]^+$. Differences in path B between HDEHP and HDHP may therefore appear only from intrinsic ligand reactivity.

Path B has been investigated through quantum chemistry calculations in order to investigate further the proposed mechanism. Calculations were first performed for the free ligands and then for $[Eu(LH)_2L_2]^+$ complexes.

For the free ligands, the fragmentation path was investigated for the protonated ligands (HDEHP and HDHP) and for the deprotonated ligands ($DHEP^-$ and DHP^-). The structures and energies along the reaction path, corresponding to the reactant, product and transition state, have been determined. The results are presented on Fig. 7. A transition state has been located corresponding to an elongation of the reactive carbon–hydrogen bond and to an elongation of the oxygen–carbon bond and leading to the alkene formation. According to the calculation, the reaction is thermodynamically favorable for di 2-ethylhexylphosphoric acid (HDEHP and $DEHP^-$, $\Delta G^0 = -2$ kcal/mol), whereas it is slightly unfavorable for di *n*-hexylphosphoric acid (HDHP and DHP^-, by 3 and 1 kcal/mol respectively). The energy barrier $\Delta G^{\ddagger}$ leading to the alkene formation is lower for the protonated ligands HDEHP and HDHP than for $DEHP^-$ and DHP^- (by 12 and 10 kcal/mol respectively) and is lower for di 2-ethylhexylphosphoric acid than for di-*n*-hexylphosphoric

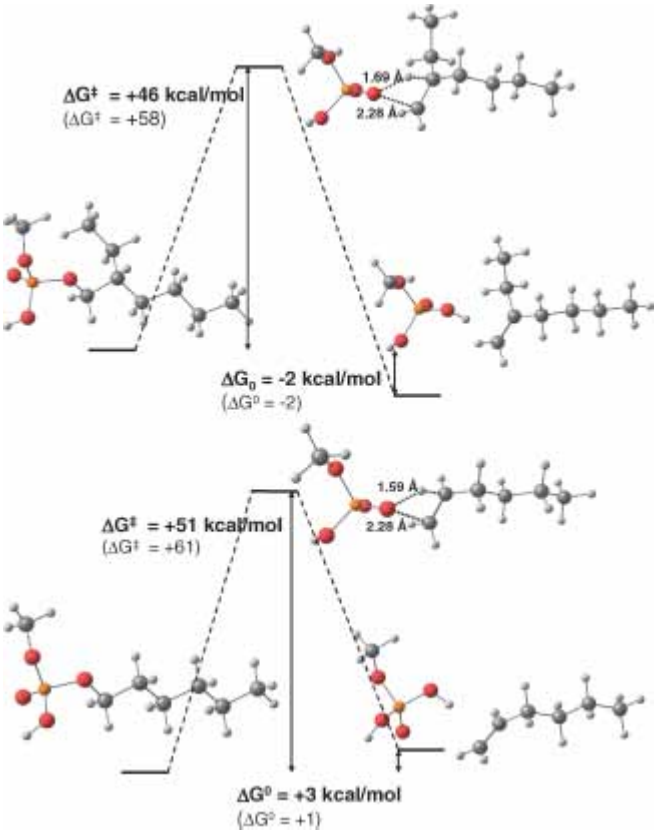

Fig. 7. Energy profiles and optimized structures corresponding to the formation of alkenes from the free ligands HDEHP (*top*) and HDHP (*bottom*) determined from DFT calculations. One of the two alkyl chains is modeled by a methyl group. Free energy variations given in parentheses correspond to $DEHP^-$ and DHP^-.

acid. According to the DFT calculations, fragmentation of the alkyl chain is both kinetically and thermodynamically slightly more favorable for HDEHP than for HDHP and is kinetically slightly more favorable for the protonated form than for the deprotonated form of the ligands.

In $[Eu(LH)_2L_2]^+$, only the fragmentation of one alkyl chain belonging to HDEHP or HDHP has been considered.

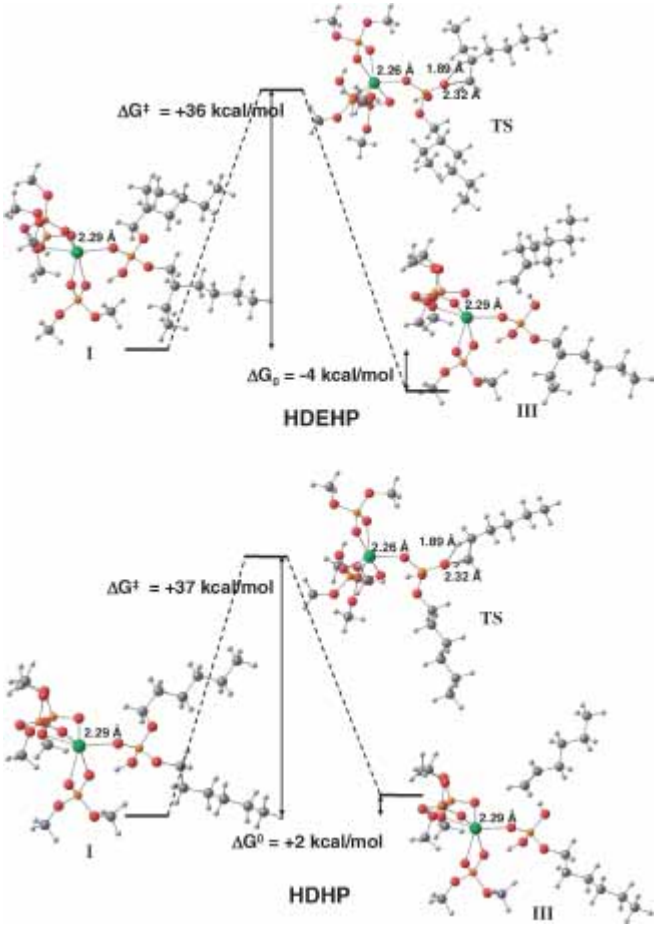

Fig. 8. Energy profiles and optimized structures corresponding to fragmentation pathway B for $[Eu(LH)_2L_2]^+$ determined from DFT calculations, HDEHP (*top*) and HDHP (*bottom*).

As described in computational details section, three of the four ligands have been modeled by di-methylphosphoric acid. The results are presented on Fig. 8. In the initial and final structures of the complexes, the distance between europium and oxygen atom from the ligand is equal to 2.29 Å for both ligands. The transition state structures are very similar to those obtained the free ligands. For HDEHP complex, the reaction is thermodynamically favorable ($\Delta G^0 = -4$ kcal/mol) whereas it is slightly unfavorable for HDHP complex ($\Delta G^0 = +2$ kcal/mol). The energy barrier $\Delta G^{\ddagger}$ is 10 to 14 kcal/mol lower than for the free ligand and is similar for both ligands. These results are in very good agreement with the fragmentation mass spectra, which indicate that the formation of an alkene is only observed for HDEHP and not for HDHP in $[M(LH)_2L_2]^+$ complexes. The difference between the two ligands is due to thermodynamic differences between the formation of 2-ethylhexene from 2-ethylhexyl alkyl chain and hexene from hexyl alkyl chain. It should be mentioned that absolute reaction energies maybe slightly shifted by changing the calculation details such as using a different functional. Previous theoretical studies have shown that energy reactions corresponding to C–H bond activation by organolanthanides can be reproduced by B3LYP calculations within a few kcal/mol [38]. In the present study, a very good accuracy can be expected on the relative energies between HDEHP and HDHP complexes whereas absolute ΔG^0 may be determined with an error of a few kcal/mol.

Conclusion

We have used electrospray ionization-mass spectrometry and theoretical chemistry calculations to investigate europium and neodymium complexes with di-2-ethylhexylphosphoric and di-*n*-hexylphosphoric acids. Electrospray ionization–mass spectrometry results reveal that europium and neodymium are surrounded by 6 ligands, which agree with previous studies in solution [9, 14, 19, 20]. The predominant species in gas phase correspond to 1 : 4 complexes where the cation is bound to two neutral and two charged ligands. 1 : 5 and 1 : 6 complexes are also observed, but they appear with a significantly lower intensity on the mass spectra.

Fragmentation mass spectra have been recorded in order to compare the binding strength between the two phosphoric acids and the stability of the complexes. Two fragmentation path are in competition, the loss of a ligand or the loss of an alkyl chain. For complexes of higher stoichiometry, $[M(LH)_4L_2]^+$ and $[M(LH)_3L_2]^+$, only one fragmentation path is observed for both ligands: a loss of a ligand. For the predominant 1 : 4 species ($[M(LH)_2L_2]^+$), both fragmentation paths take place with di-2-ethylhexylphosphoric acid, whereas only the loss of a ligand is observed for di-*n*-hexylphosphoric acid complexes.

According to molecular dynamic simulations performed on europium complexes, the loss of one ligand (path A) is energetically equivalent for both ligands at each $[Eu(LH)_nL_2]^+$ stoichiometry but the energy required decreases when the stoichiometry increases.

From quantum chemistry calculations, it appears that the fragmentation of the alkyl chain into an alkene (path B) is thermodynamically more favorable for di-2-ethylhexylphosphoric than for di-*n*-hexylphosphoric acid (by 6 kcal/mol for $[Eu(LH)_2L_2]^+$ complexes). The results of the calculations are in very good agreement with those obtained from fragmentation mass spectra and we can conclude that the lanthanide-ligand binding strength is similar between the two ligands whereas the di-2-ethylhexyl chain is less stable than the *n*-hexyl chain toward alkene formation. Moreover, the reaction path leading to the alkene formation has been investigated for the free phosphoric acids and compared to the results obtained for the europium complex. The results of calculations reveal that the alkene formation from the alkyl chain is becoming kinetically more favorable upon binding to the lanthanide ion.

In conclusion, we note that ionization-mass spectrometry is a valuable approach to obtain structural information on the complexes form during solvent extraction experiments and that combining theoretical calculations and ESI-MS can bring quantitative information on the stability of the complexes.

References

1. Choppin, G., Liljenzin J.-O., Rydberg, J.: *Radiochemistry and Nuclear Chemistry*. 3rd Edn., Butterworth-Heinemann, Woburn (2002), chapt. 21, p. 624.

2. Madic, C., Hudson, M. J., Liljenzin, J.-O., Glatz, J.-P., Nannicini, R., Facchini, A., Kolarik, Z., Odoj, R.: Prog. Nucl. Energy **40**, 523 (2002).
3. Hérès, X., Nicol, C., Bisel, I., Baron P., Ramain, L.: Proceedings of the International Conference on Future Nuclear Systems, Global'99: Nuclear Technology – Bridging the Millennia, Jackson Hole, WY, USA, Aug. 29–Sept. 3 (1999), p. 585.
4. Baron, P., Rostaing-Nicol, C., Hill, C., Hérès, X., Camès, B., Berthon, L., Roussel, H., Guilbaud, P., Lecomte, M., Masson, M., Dancausse, J. P., Calor, J. N., Ferlay G., Madic, C.: Atalante: Rapport Scientifique, CEA-R-6800 (2002), p. 76.
5. Charbonnel, M. C., Berthon, L.: Direction du Cycle du Combustible: Rapport Scientifique, CEA-R-5801 (1997), p. 114.
6. Serrano-Purroy, D., Christiansen, B., Glatz J. P., Malmbeck, R., Modolo, G.: Radiochim. Acta **93**, 357 (2005).
7. Gannaz, B.: Thèse de Doctorat de l'Université Paris XI, Paris, France (2006).
8. Nash, K. L.: Solvent Extr. Ion Exch. **11**, 729 (1993).
9. Gannaz, B., Chiarizia, R., Antonio, M. R., Hill, C., Cote, G.: Solv. Extr. Ion Exch. **25**, 313 (2007)
10. Marcus, Y., Kertes A. S.: *Ion Exchange and Solvent Extraction of Metal Complexes*. Wiley-Interscience, New York (1969) p. 521
11. Kolarik, Z., Sistkova, N. A., Hejna, J.: *Solvent Extraction Research*. (Kertes, A. S., Marcus, Y., eds.) Wiley-Interscience, New York (1969), p. 59.
12. Kolarik, Z.: Pure Appl. Chem. **54,** 2593 (1982)
13. Ulyanov, V. S., Sviridova, R. A.: Sov. Radiochem. **12,** 41 (1970).
14. Yoshizuka, K., Kosaka, H., Shinohara, T., Ohto, K., Inoue, K.: Bull. Chem. Soc. Japan. **69**, 589 (1996).
15. Buch, A., Stambouli, M., Pareau, D., Durand, G.: Solv. Ext. Ion Exch. **20**, 49 (2002).
16. Biswas, R. K., Banu, R. A., Islam, M. N.: Hydrometallurgy **69**, 157 (2003).
17. Peppard, D. F., Ferraro, J. R.: J. Inorg. Nucl. Chem. **10**, 275 (1959).
18. Hardy, C. J., Scargill, D.: J. Inorg. Nucl. Chem. **17**, 337 (1961).
19. Jensen, M. P., Chiarizia, R., Urban, V.: Solv. Extr. Ion Exch. **19**, 865 (2001).
20. Gannaz, B., Antonio, M. R., Chiarizia, R., Hill, C., Cote, G.: Dalton Trans. 4553 (2006).
21. Traeger, J. C.: Int. J. Mass Spectrom. **200**, 387 (2000).
22. Daniel, J. M., Friess, S. D., Rajagopalan, S., Wendt, S., Zenobi, R.: Int. J. Mass Spectrom. **216**, 1 (2000).
23. Di Marco V. B., Bombi G. G.: Mass Spectrom. Rev. **25**(3), 347 (2006).
24. Krabbe, J. G., de Boer, A. R., van der Zwan, G.; Lingeman, H.: J. Am. Soc. Mass Spectrom. **18**, 707 (2007).
25. Stewart I. I., Horlick, G.: Anal Chem. **66**, 3983 (1994).
26. Delangle, P., Husson, C., Lebrun, C., Pécaut, J., Vottero, J. A.: Inorg. Chem. **40**, 2953 (2001).
27. Colette, S., Amekraz, B., Madic, C., Berthon, L., Cote, G., Moulin, C.: Inorg. Chem. **41**, 7031 (2002).
28. Colette, S., Amekraz, B., Madic, C., Berthon, L., Cote, G., Moulin, C.: Inorg. Chem. **42**, 2215 (2003).
29. Crowe, M. C., Kapoor, R. N., Cervantes-Lee, F., Parkanyi, L., Schulte L., Pannell, K. H., Brodbelt, J. S.: Inorg. Chem. **44**, 6415 (2005).
30. Lamouroux, C., Moulin, C., Tabet, J. C., Jankowski, C. K.: Rapid Commun. Mass Spectrom. **14**, 1869 (2000).
31. Lamouroux, C., Rateau, S., Moulin, C.: Rapid Commun. Mass Spectrom. **20**, 2041 (2006).
32. HDHP was synthesized by S. Garcia-Argote, CEA-Valrhô, DEN/VRH/DRCP/SCPS/LCAM.
33. Frisch, M. J., Trucks, G. W., Schlegel, H. B., Scuseria, G. E., Robb, M. A., Cheeseman, J. R., Zakrzewski, V. G., Montgomery Jr., J. A., Stratmann, R. E., Burant, J. C., Dapprich, S., Millam, J. M., Daniels, A. D., Kudin, K. N., Strain, M. C., Farkas, O., Tomasi, J., Barone, V., Cossi, M., Cammi, R., Mennucci, B., Pomelli, C., Adamo, C., Clifford, S., Ochterski, J., Petersson, G. A., Ayala, P. Y., Cui, Q., Morokuma, K., Malick, D. K., Rabuck, A. D., Raghavachari, K., Foresman, J. B., Cioslowski, J., Ortiz, J. V., Baboul, A. G., Stefanov, B. B., Liu, G., Liashenko, A., Piskorz, P., Komaromi, I., Gomperts, R., Martin, R. L., Fox, D. J., Keith, T., Al-Laham, M. A., Peng, C. Y., Nanayakkara, A., Challacombe, M., Gill, P. M. W., Johnson, B., Chen, W., Wong, M. W., Andres, J. L., Gonzalez, C., Head-Gordon, M., Replogle E. S., Pople, J. A.: Gaussian98, Gaussian Inc., Pittsburgh PA (1998).
34. Dolg, M., Stoll, H., Preuss, H.: Theor. Chim. Acta **85**, 441 (1993).
35. Case, D. A., Pearlman, D. A., Caldwell, J. W., Cheatham III, T. E., Ross, W. S., Simmerling, C. L., Darden, T. A., Merz, K. M., Stanton, R. V., Cheng, A. L., Vincent, J. J., Crowley, M., Tsui, V., Radmer, R. J., Duan, Y., Pitera, J., Massova, I., Seibel, G. L., Singh, U. C., Weiner, P. K., Kollman, P. A.: AMBER 6, University of California, San Francisco (1999).
36. Durand, S., Dognon, J.-P., Guilbaud, P., Rabbe C., Wipff, G.: J. Chem. Soc. Perkin Trans. **2**, 705 (2000).
37. Cornell, W. D., Cieplak, P., Bayly, C. I., Kollman, P. A.: J. Am. Chem. Soc. **115**, 9620 (1993).
38. Sherer, E. C., Cramer, C. J.: Organometallics **22** 1682 (2003)